RevMexAA (Serie de Conferencias), **28**, 17–23 (2007)

INTEGRAL FIELD SPECTROSCOPY FOR PANORAMIC TELESCOPES

Jeremy Allington-Smith[1]

RESUMEN

Revisaremos los principios básicos de la espectroscopía de campo integral usando la densidad específica de información como un parámetro objetivo de comparación. De esta forma se muestra que el mejor método en teoria es el rebanador de imagenes, especialmente como está implementado en el diseño del Rebanador de Imagen Avanzado usado en la Unidad de Campo Integral del Espectrógrafo Gemini para el Mediano Infrarrojo. Una alternativa que podría ofrecer un mejor compromiso entre el rendimiento teórico y el funcionamiento práctico para estudios espectroscópicos panorámicos que requieren millones de elementos espaciales, como es el caso del proyecto de telescopios gemelos en San Pedro Mártir, sería un híbrido de arreglo sin lentes con técnicas de rebanador. Ya existen diseños conceptuales de este tipo, como el que se planea para el espectrógrafo IMACS del Magallanes.

ABSTRACT

The basic principles of integral field spectroscopy are reviewed using a figure of merit, the specific information density, as an objective means of comparison. This shows that the best method in theory is image slicing, especially as implemented in the Advanced Image Slicer design used in the Integral Field Unit of the Gemini Near-Infrared Spectrograph. However, an alternative, a hybrid of lenslet array and slicer techniques, may offer a better compromise between theoretical performance and practicality for panoramic spectroscopic surveys requiring millions of spatial elements such as the San Pedro Mártir twin telescope project. Conceptual designs of this type already exist, including one aimed at the IMACS spectrograph on Magellan.

Key Words: **INSTRUMENTATION: SPECTROGRAPHS — TECHNIQUES: SPECTROSCOPIC**

1. GENERAL

The term 3D spectroscopy is often used for any technique that produces spatially-resolved spectra over a two-dimensional field. Integral field spectroscopy is that subset of “3D spectroscopy” in which all the data for one pointing of the telescope are obtained simultaneously. The other methods, such as Fabry-Perot Interferometry (FPI) and Imaging Fourier Transform Spectroscopy (IFTS) use the time domain to step through wavelength space (or a Fourier conjugate). This leaves them potentially sensitive to changes in the instrumental or sky background, but allows a wide field to be covered in one pointing. In contrast, Integral Field Spectroscopy (IFS) encodes all the spectral and spatial information in the same exposure, resulting in a smaller field of view for a given detector format.

Although this paper deals mostly with IFS, the important contribution played by non-IFS 3D instrumentation must be acknowledged. Radio astronomers were making 3D spectral imaging observations long before it was adopted seriously in the optical regime and FPI and IFTS have an illustrious history that predates most IFS work and are well-suited to many areas of investigation.

All 3D techniques produce a datacube of a scalar quantity related to flux density as a function of spatial coordinates in the field and wavelength. To first order, the efficiency of all 3D techniques is the same. For example, IFTS may provide a large number of spatial samples (spaxels) at one time but require a large number of timesteps to scan through the spectrum. IFS may produce all the spectral information in one exposure, but its field of view is necessarily limited so that a number of exposures with different pointings must be mosaiced to produce the same number of volume resolution elements (voxels). The same argument applies to stepped-longslit spectroscopy: each position provides full spectral information for a 1D line of spaxels but a number of separate exposures must be combined to cover the same 2D field as the other techniques discussed. To second order, the relative efficiency of the techniques differ, depending on the details of how data from different exposures are combined, the variability of the background compared to fixed noise sources, and the nature of the required data product.

[1]Centre for Advanced Instrumentation, Physics Department, Durham University, South Road, Durham DH1 4RJ, UK (j.r.allington-smith@durham.ac.uk).

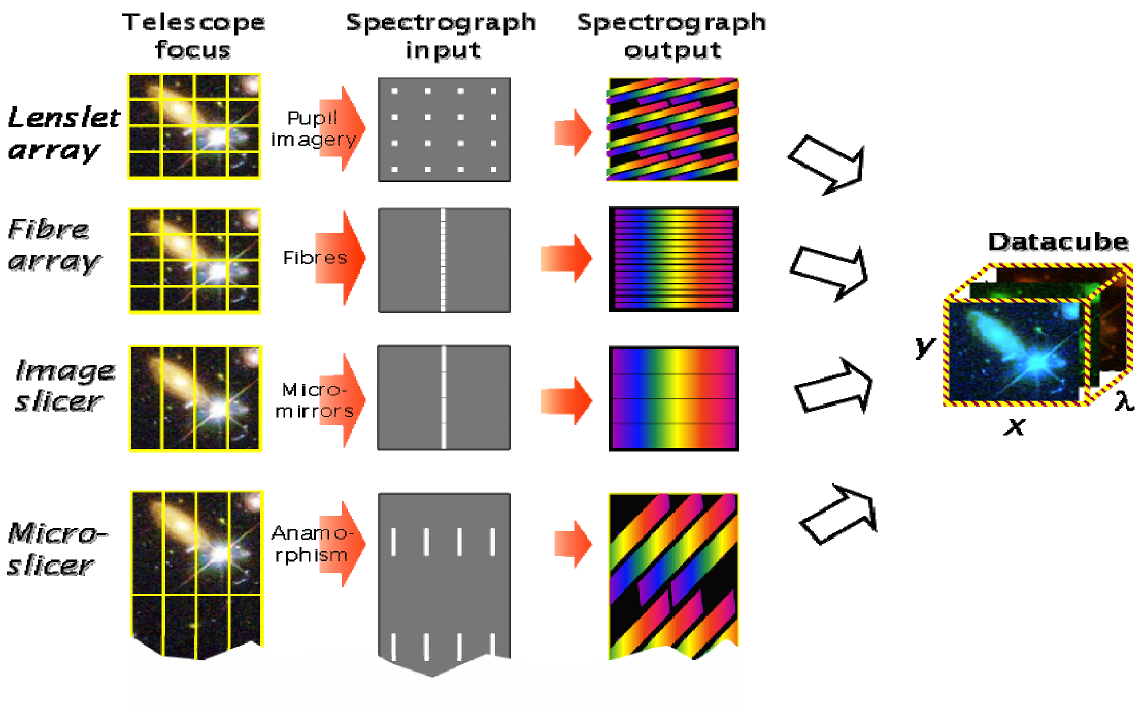

Fig. 1. A summary of the four main techniques of integral field spectroscopy.

3D techniques are generally preferable to slit spectroscopy for a number of reasons: (a) slit losses are eliminated; (b) accurate target acquisition is not required; (c) the actual target position can be recovered from the data by reconstructing an image — also an aid to accurate mosaicing; (d) errors in radial velocity due to differences in the barycenter of the slit illumination obtained from the object and from reference sources can be eliminated; (e) the global velocity field is recovered without bias imposed by the observer's choice of slit position and orientation; (f) atmospheric dispersion effects can be corrected without loss of light by manipulation of the datacube; (g) in poor or variable seeing, IFS is always optimally matched to the object PSF.

2. THE DIFFERENT METHODS OF IFS

Figure 1 summarizes four techniques of IFS; see Allington-Smith (2006a) for more detail. The fourth of these techniques is a recent idea proposed by Content (2006) as a means to provide ∼1 million spaxels to search for primeval galaxies.

It useful to define a figure of merit (FOM): the specific information density (SID)

$$Q = \eta \frac{N_p N_q N_\lambda}{N_x N_y} \qquad (1)$$

where N_p and N_q are the numbers of spatial resolution elements in orthogonal directions p and q in the field. These quantities are related to the numbers of spaxels via $N'_p = N_p f_s$, $N'_q = N_q f_s$ where f_s is the oversampling of the PSF by the *IFU*. N_λ is the number of spectral resolution elements which is related to the number of spectral samples by $N'_\lambda = N_\lambda f_\lambda$ where f_λ is the spectral oversampling by the *detector*. N_x and N_y are the numbers of pixels in the detector in orthogonal directions x and y, and η is the throughput of the IFU[2]. The coordinates, x and y are aligned with directions p and q on the sky in the sense that p is the dimension that varies most rapidly along the slit which is defined by the detector y direction.

Although Q is a useful FOM for comparing different IFS systems, a comparison of different 3D techniques requires a more general metric such as $Q/n_e t_e$ where n_e is the number of separate exposures and t_e is the duration of each.

The theoretical maximum SID is obtained when $N'_p N'_q N'_\lambda = N_x N_y$; for Nyquist sampling ($f_s = f_\lambda = 2$) $Q_{max} = 1/8$. The case of super-sampling, by combining exposures with offsets of non-integral numbers of pixels, can be handled using this formalism by considering the combined observation to have been

[2] Throughput is measured from the IFU's input to its output but including losses at the spectrograph stop. Alternatively, it is measured by comparison with the same spectrograph using a single slit of the same equivalent width.

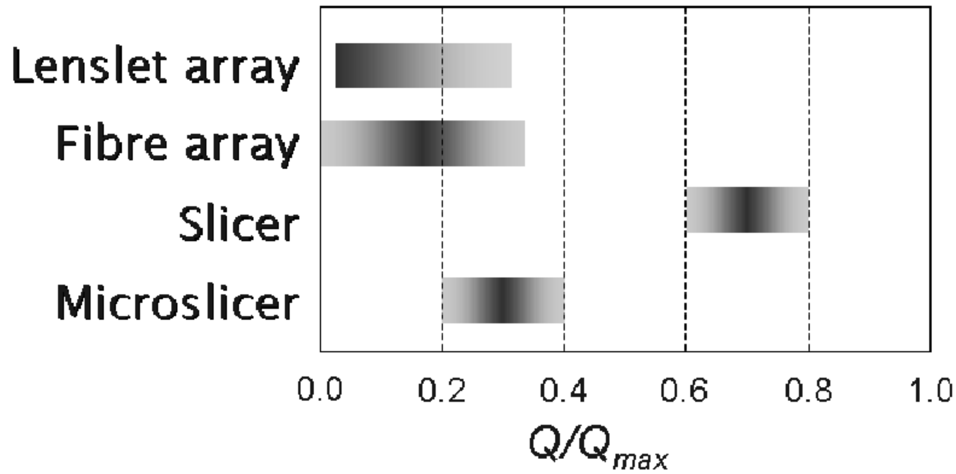

Fig. 2. A comparison of the Specific Information Density (normalized to the theoretical maximum) obtainable with existing IFS instrumentation. Although based on calculations of specific instruments, a greyscale is used to indicate the range and barycenter of the distribution generally available.

obtained with a virtual instrument with enhanced resolution. However, the number of separate exposures will then need to be accounted for via the $Q/(n_e t_e)$ metric used for generalized 3D instruments.

The advantage of the SID as a FOM is that it is simply a measure of the *information content per detector pixel* and is thus appropriate for a discussion of cost-limited instrumentation whereas a FOM based on signal-to-noise is appropriate for discussion of specific astrophysical studies. SID makes no assumption about the contiguity of the spaxels within the field or the size of the field and so does not discriminate against sparsely-sampled IFS where contiguity is sacrificed for field (e.g., to measure the surface gravity over a face-on disk galaxy). Likewise, by defining the SID in terms of *resolution* elements rather than *sampling* elements, the statistical correlation between samples is naturally taken into account: it is only necessary to convert correctly between resolution elements and samples. The correlation may arise from (the normally desirable) oversampling according to the Nyquist theory of an image conjugate, or from crosstalk elsewhere in the instrument, e.g., at the slit. The correlations may be absent in the case of sparse sampling.

Expressions for the SID for each of the four techniques identified are given in Allington-Smith (2006a) in terms of instrumental parameters such as the spaxel-to-spaxel pitch on which the samples are imaged on the detector and the number and size of the gaps required to prevent cross-talk between statistically-independent regions of the sky.

Figure 2 presents a comparison of the different techniques. The SID of each technique covers a wide range because of differences in the design of some types of instrument. For example, the Keck OSIRIS (Larkin et al. 2006) has achieved an unusually high SID for a lenslet array IFS (e.g., Bacon et al. 2001) because the design strives to pack the pupil images as close together as possible. However, as noted above, the SID does not take into account any influence that the close-packing of the spectra might have on the recoverable signal-to-noise. This consideration also highlights the essential role played by the data reduction software in optimizing scientific return.

This comparison shows the near-optimal potential performance of image slicers (Weitzel et al. 1996). However, the other techniques are broadly similar to each other, including the recent generation of lenslet-only devices which might naively be thought to be at a disadvantage because of the lack of reformatting. The new micro-slicer technique is well-suited to devices with very large numbers of spaxels, since it makes uses of easily-replicable anamorphic lenslet arrays rather than complex figured mirrors; it is encouraging that this has the potential to reach moderately-high SID.

3. ISSUES FOR SLICING IFUS

3.1. *Performance challenges for image slicers*

Results from early devices such as the Gemini Near Infrared Spectrograph (GNIRS) IFU (Allington-Smith et al. 2004, 2006b) using the Advanced Image Slicer (AIS) principle (Content 1997)

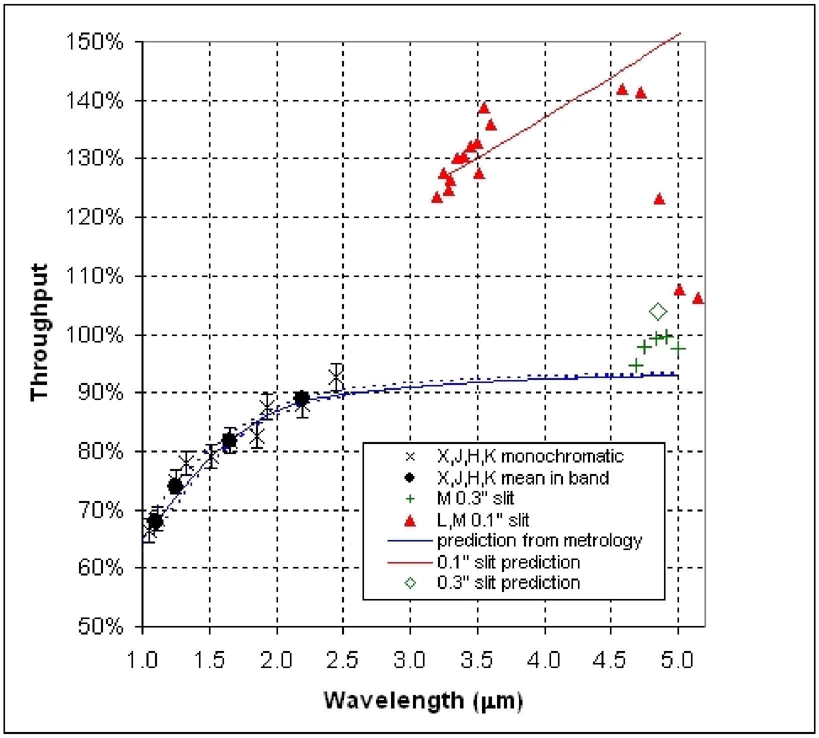

Fig. 3. The throughput of the GNIRS-IFU as a function of wavelength. The prediction assumes that the only loss mechanism is the reflectivity of the gold-coatings (almost independent of wavelength) and the total integrated scatter due to surface roughness. The prediction is calculated using measurements of the roughness as manufactured and refers to the part of the IFU which maps onto the extent of the GNIRS longslit, excluding a small damaged portion of one slice. The throughput represents the ratio of the throughput of the spectrograph with the IFU deployed and with the IFU replaced with a slit of twice the slice width. Results for a narrower slit are also shown after scaling to the same effective slitwidth to show how the IFU is better able to cope with diffracted light than the traditional slit, resulting in an apparent efficiency exceeding unity.

demonstrate excellent performance. Compared to the original design, the AIS brings the benefit of square spaxels, greater immunity to diffraction loss, smaller size, and easier optical interfaces at the expense of greater complexity on the surface forms of the constituent mirrors (see summary by Allington-Smith 2006). The throughput (Figure 3) is determined, (apart from a small loss due to the non-unit reflectivity of the gold coating) exclusively by the roughness of the optical surfaces. For GNIRS, this was $\sigma = 15$–20 nm.

Although superior at all wavelengths to similar fiber-based IFUs in the optical, it is clear that smoother optics are required in the future especially if these devices are to be used at visible wavelengths as an alternative to lenslet and fiber systems. This is shown in Figure 4 where the as-built performance of the GNIRS-IFU is compared with predictions for a similar system (with 6 optical surfaces) but with improved surface finish. It should be noted that surface reflectivity does become a major factor at shorter wavelengths where gold cannot be used. From this it seems that *rms* roughness of better than $\sim$5 nm is required for reasonable efficiency in the visible. Even in the infrared, good surface quality is required. For example, KMOS (Sharples et al. 2004; Sharples 2006) requires $\sigma = 10$ nm.

This is probably achievable using the diamond-machined aluminum approach employed in GNIRS, but may need to be augmented by post-polishing. Trials suggest (J. Schmoll, private comm.) that the initial surface may be improved by a factor of two in this way. An alternative is to polish glass mirrors using traditional techniques which are then assembled and aligned individually to high accuracy (Laurent et al. 2006) in contrast to the machined-metal approach which seeks to eliminate inter-facet alignment problems by making monolithic arrays of facets (Schmoll

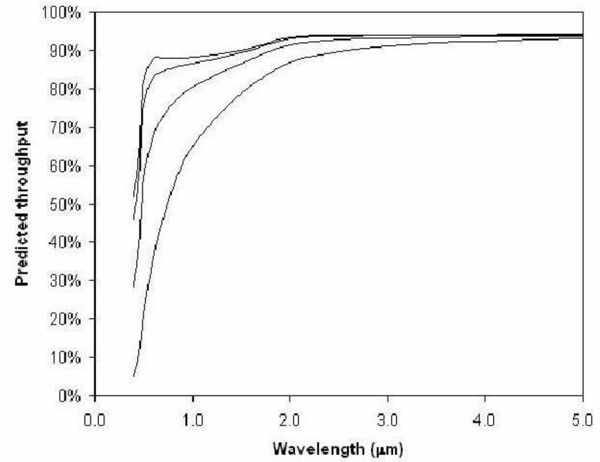

Fig. 4. Predicted throughput for the IFU obtained from the performance model shown in Figure 1 (bottom curve) and predictions for an *rms* surface roughness of 2, 5, 10 nm, respectively, from top to bottom. For wavelengths shorter than 1 μm, the reflectivity of silver has been used since gold ceases to be effective. Aluminum is assumed at 0.4μm.

et al. 2006; Preuss & Rickens 2006; Dubbeldam et al. 2004, 2006).

A second issue for image slicers is the complexity of the optical system. Although the number of separate optical prescriptions can be reduced and aspheric surfaces largely avoided (but some toroids are generally required), and monolithic construction adopted to greatly simplify the assembly, the number of pieces to be made is daunting, roughly $3+3N_S$ for N_S slices for each IFU, equaling 66 for the modest GNIRS-IFU. For a survey system based on this system, the numbers will be vast with $N_S \approx \sqrt{N_p' N_q'}$ requiring $3N_I + 3\sqrt{N_p' N_q'}$ if the spaxels are distributed between N_I IFUs. For a modular system, the prescriptions need not be unique. If the spaxels are divided between a number of identical spectrographs, the number of unique prescriptions is reduced by that factor.

Production engineering is more commonly suited to the manufacture of TVs or cars, but its principles — with emphasis on testing strategies — may be applied to the production of astronomical instrumentation. It is not yet clear if replication techniques can be used successfully while maintaining good surface quality.

3.2. *Potential of Micro-slice IFUs*

Although delivering lower SID, microslicing IFUs can be made from standardized components made by replication from a small number of masters. Figure 5 shows further detail of the micro-slice design concept. Two pairs of crossed-cylindrical lenslets or a pair of rectangular arrays are used in conjunction with anamorphic fore-optics to divide the field into rectangles. These rectangles are then shrunk into sliced images which contain no spatial information in the dispersion direction — as with the original lenslet array technique — but retain spatial information in the spatial direction along the slice.

Designs exist for IFUs with millions of spaxels as shown in Table 1 taken from Content (2006). This table includes a design suitable for use with the Magellan IMACS instrument which is described by Content as follows:

> "IMACS is a multi-object spectrograph using slit masks in the input focal plane. It has an 8k x 8k detector. An IFU designed and built by our group can also be placed in the focal plane. It is a fiber-lens IFU similar to the GMOS IFUs with 2 fields of 1000 lenslets (Schmoll et al. 2004). A microslice IFU could also be used. With the short camera, it would cover nearly $3' \times 3'$ if we accept spectra about 100 pixels long only (Figure 4). This would give about 400,000 spaxels, far more than the 2000 of our fiber-lens IFU but at the price of far shorter spectra."

Further details are given in Content (2006). In the table, values in parentheses are for the IMACS long camera with a high resolution grating.

4. CONCLUSIONS: IMPLICATIONS FOR PANORAMIC SURVEY TELESCOPES

Panoramic IFS surveys such as those envisaged for the San Pedro Mártir telescopes clearly require vast numbers of spaxels. Although the slicing IFUs deliver better SID than arrays, there remain questions over their implementation on such a large scale.

These two methods have their relative merits; the optimum choice being, as ever, dependent on the details of the astrophysical investigation and the operational environment (e.g., terrestrial/space and warm/cold).

The alternative is to use micro-slicing which requires standardized components which can be (and must be) made by replication from a small number of masters. The SID is reduced by a factor of 2–3, but the system will be easier and cheaper to build.

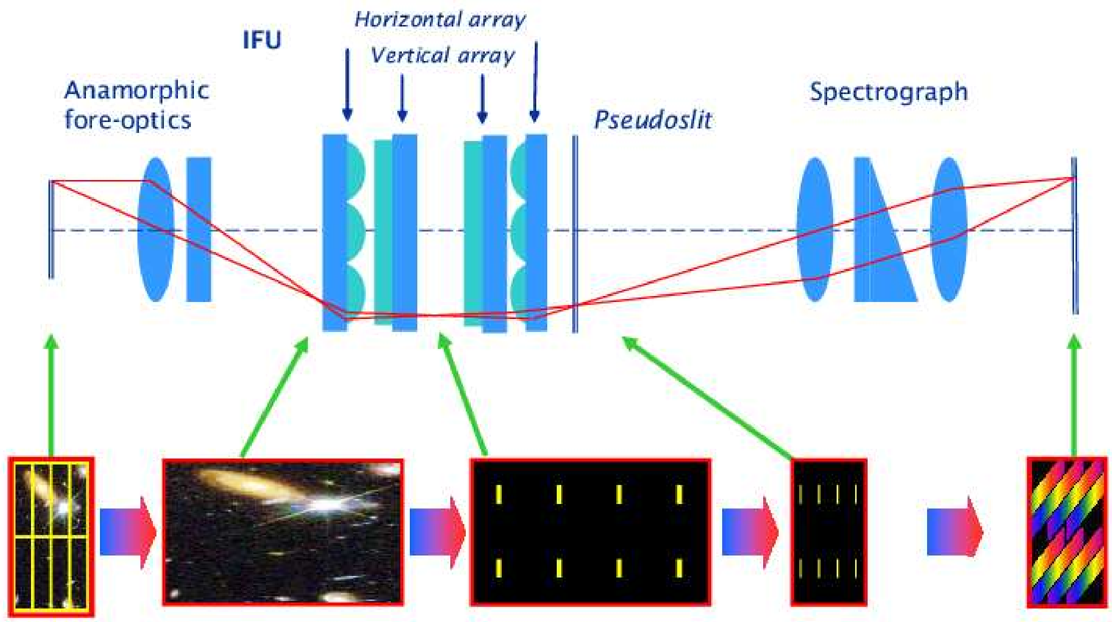

Fig. 5. Microslice concept realized using lenslet arrays and anamorphic fore-optics. Adapted from Content (2006).

TABLE 1

SUMMARY OF MICRO-SLICE DESIGNS (FROM CONTENT 2006).

	8-m MEIFUS	ELT MEIFUS	IMACS P4MEIFU
Spatial resolution (arcsec)	0.15 x 0.30	0.1 x 0.2	0.2 x 0.4 (0.11 x 0.4)
Total field (arcmin)	5.2 x 5.2	2.7 x 3.0	3.0 (1.7 x 3.0)
Number of spatial elements (Million)	2.2	1.5	0.4
Spectral length (pixel)	200	600	100
Number of spectrographs	16	24	1
Spectral resolution	500 and 1500	1800	3000 (20,000)

Further work is required to establish the feasibility of micro-slicing systems. Although several designs exist, none has yet been built.

The different methods of IFS have been compared using an appropriate figure of merit: the specific information density. From this it can be seen that image slicers approach the theoretical maximum performance. However, the complexity of such devices for very large formats may prove problematic and require hybrid alternatives which are easier to build even if they do offer the same level of theoretical performance. This consideration is highly relevant to the proposed San Pedro Mártir telescopes which are predicated on massive use of IFS.

The Centre for Advanced Instrumentation of Durham University is actively pursuing a vigorous program to develop image slicer technology, addressing both the surface finish and complexity issues, and has been selected to manufacture, with SIRA Ltd, the IFU for the JWST NIRSpec instrument. The alternative micro-slicer paradigm has also been developed by the Centre for Advanced Instrumentation.

Many thanks to Robert Content for patiently explaining his many innovations to me so that I can discuss them here. Thanks too, to Graham Murray, Jürgen Schmoll and Marc Dubbeldam for their huge and successful endeavors in producing the GMOS, IMACS and GNIRS IFUs.

REFERENCES

Allington-Smith, J., Dubbeldam, C. M., Content, R., Dunlop, C., Robertson, D. J., Elias, J., Rodgers, B., & Turner, J. E, 2004, Proc. SPIE, 5492, 701

Allington-Smith, J. R. 2006a, NewARev, 50, 244

Allington-Smith, J., Dubbeldam, C. M., Content, R., Robertson, D. J., & Preuss, W. 2006b, MNRAS, 371, 380

Bacon. R., et al. 2001, MNRAS, 326, 23

Content, R. 1997, Proc. SPIE, 2871, 1295

Content, R. 2006, NewARev, 50, 267

Dubbeldam, C. M., Robertson, D. J., & Preuss, W. 2004, Proc. SPIE, 5494, 163

Dubbeldam, C. M. 2006, NewARev, 50, 342

Larkin, J., et al. 2006, NewARev, 50, 362

Laurent, F., et al. 2006, NewARev, 50, 346

Preuss, W., & Rickens, K. 2006, NewARev, 50, 332

Schmoll, J., et al. 2006, NewARev, 50, 263

Sharples, R. M., et al. 2004, Proc. SPIE, 5492, 1179

Sharples, R. M. 2006, NewARev, 50, 443

Weitzel, L., Krabbe, A., Kroker, H., Thatte, N., Tacconi-Garman, L. E., Cameron, M., & Genzel, R. 1996, A&AS, 119, 531